Geophys. J. Int. (2003) **152,** 335–343

Rock magnetic record of the last glacial–interglacial cycle from the Kurtak loess section, southern Siberia

R. X. Zhu,[1] G. Matasova,[2] A. Kazansky,[2] V. Zykina[2] and J. M. Sun[1]

[1] *Palaeomagnetism Laboratory, Institute of Geology and Geophysics, Chinese Academy of Sciences, Beijing* 100101, *China. E-mail: rxzhu@mail.c-geos.ac.cn*
[2] *Institute of Geology, UIGGM Siberian Division, Russian Academy of Sciences, Novosibirsk, Russia*

Accepted 2002 August 5. Received 2002 June 13; in original form 2001 October 10

SUMMARY

Detailed rock magnetic investigations, grain size determination and X-ray diffraction were carried out on loess and buried soils of the last glacial–interglacial cycle from Kurtak, southern Siberia. The susceptibility and the sand fraction of >63 μm fluctuate in parallel, suggesting that the higher susceptibility values in the loess horizons are mainly associated with the coarse size fraction. The frequency dependence of the magnetic susceptibility of the loess and buried soils is very low and uniform, indicating the absence of superparamagnetic grains and negligible pedogenically induced enhancement of magnetic susceptibility. The magnetic assemblage is dominated by multidomain-like magnetite grains. Maghemite and haematite are also present in the buried soils and loess horizons. Goethite may have been formed from gleying or waterlogging processes under a cooler and more humid climate. The coarse magnetite grains, which contribute significantly to magnetic susceptibility, are probably carried by valley winds and derived from local sources. Thus, the coarser magnetite grains with higher susceptibility values in the loess horizons could mainly reflect stronger wind intensity during cold and semi-arid conditions, and the consequent ease with which dense magnetite particles can be transported. The lower susceptibility values in the buried soil horizons are mainly caused by weaker wind intensity during interglacial and interstadial periods, although post-depositional processes associated with gleying modifications are also partially responsible for the observations.

Key words: buried soil, loess, palaeoclimate, rock magnetism, Siberia.

1 INTRODUCTION

Since the 1980s, rock magnetic studies of the Chinese loess/palaeosol sequences have contributed significantly to our understanding of global and regional climatic and environmental changes (e.g. Heller & Evans 1995; Maher 1998; Evans & Heller 2001). It has been shown that mineral magnetic parameter profiles from different sites in the Chinese Loess Plateau show features similar to those documented in the oxygen isotope records from marine sediments (e.g. Heller & Liu 1984, 1986; Kukla *et al.* 1988), which have been interpreted as a global ice-volume signal and hence as a proxy for global climatic changes. In the previous few years, the loess deposits elsewhere in the world have also increasingly attracted attention and some excellent palaeoclimatic records have been obtained from the loess/palaeosol sequences in southern Siberia (Chlachula *et al.* 1997, 1998). The Kurtak section (55.1°N, 91.4°E) (Fig. 1) is one of the most studied loess sequences in southern Siberia (Chlachula *et al.* 1997, 1998; Matasova *et al.* 2000, 2001; Zhu *et al.* 2000). Here we report on the rock magnetic record of the last glacial–interglacial cycle from this section, which can contribute to a better understanding of the rock magnetic records of the Siberian loess deposits and their palaeoclimatic and palaeoenvironmental significance.

2 GEOLOGICAL SETTING

In southern Siberia, thick loess sediments both of aeolian origin and reworked by secondary processes cover an area of more than 700 000 km^2, between latitudes of 50° and 59°N and longitudes of 66° and 97°E (Fig. 1). During the Late Pliocene and Early Pleistocene, fluvial systems were established, accompanied by ongoing neotectonic uplift (Chlachula *et al.* 1997). The loess sediments, with thicknesses of up to 100 m, are connected with the development of the fluvial systems along the Siberian major rivers (Volkov & Zykina 1984; Frechen & Yamskikh 1999). The Kurtak section is located in the north of the Minusa intermontane depression, on top of the non-terraced gentle northern slope of the Yenisei valley (Fig. 1). Late Pleistocene subaerial deposits with thickness of approximately 21 m consist of three loess units (LE1, LE2, LE3) and three buried soils, called the Kurtak soil (SO1), Sukhoy Log soil (SO2) and Kamenny Log soil (SO3) (Fig. 2) (Arkhipov *et al.* 1992). The last glacial deposits are composed of LE1, SO1 and LE2, corresponding,

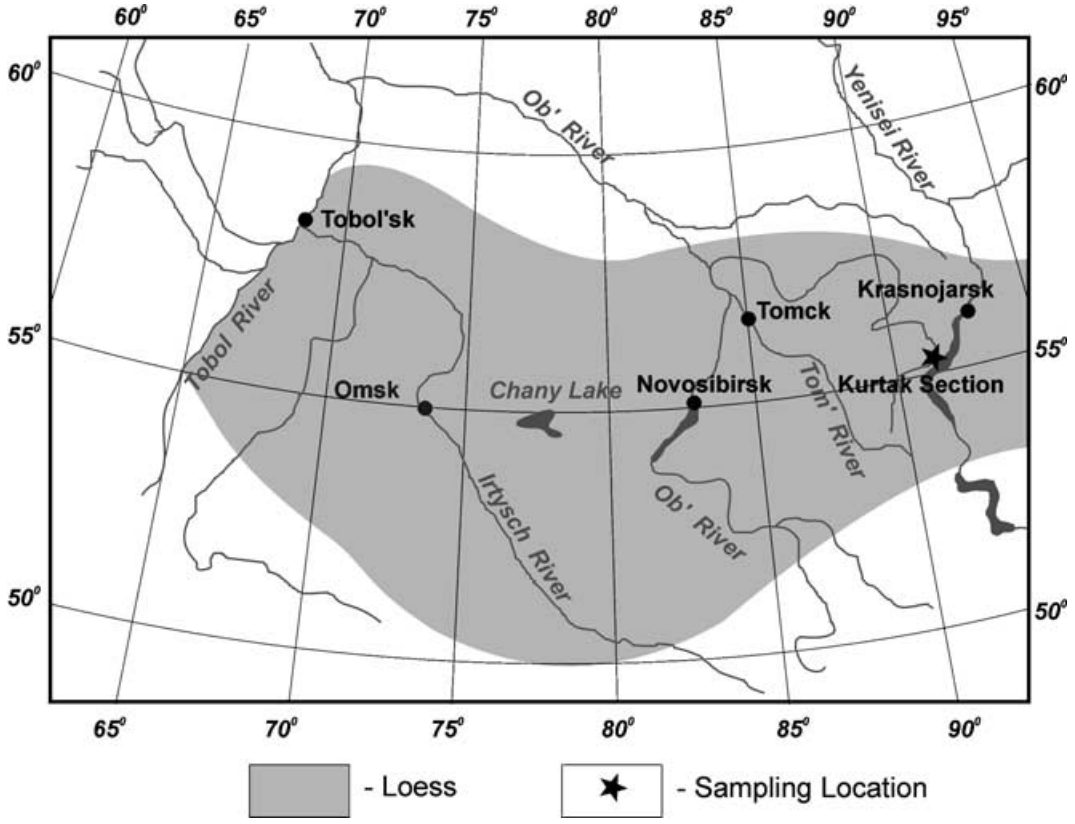

Figure 1 Distribution of loess in southern Siberia. The sampling site is indicated with a star.

respectively, to marine δ^{18}O stages (MIS) 2, 3 and 4. The last interglacial, corresponding to MIS5, produced the SO2, LE3 and SO3 layers (Fig. 2). The uppermost unit LE1 (MIS2) is a massive loess unit intercalated by colluviated regosolic tundra-steppe soils, the early last glacial loess LE2 (MIS4) mainly comprises massive aeolian loess intercalated by brunisolic forest-tundra soil horizons, while the middle last glacial buried soil SO1 (MIS3) is a chernozem soil with weakly developed humic horizons. The last interglacial pedocomplex (MIS5) mainly consists of dark brown steppe chernozems and brunisolic soils intercalated by an aeolian loess unit LE3 (Chlachula *et al.* 1997; Chlachula 2001). These loess units (or buried soils) show similar pedogenetic characteristics. In addition, some previous investigations on this section (Chlachula *et al.* 1997, 1998; Matasova *et al.* 2001) have shown that magnetic properties of the three loess units (or the three buried soils) are similar. Therefore, only loess unit LE2 and soil unit SO1 are thoroughly studied in this paper.

3 EXPERIMENTAL METHODS

Powdered samples were collected at 10 cm intervals throughout the entire section. Low-field susceptibilities of 176 samples were measured using a Bartington Instruments susceptibility meter with a MS-2B probe. The low- and high-frequency susceptibilities were measured at approximately 470 and 4700 Hz, respectively. Grain sizes of 140 samples were analysed using a computer-operated PRO-700 SK Laser Micron Sizer.

Similar to the partial heating/cooling method (Van Velzen & Dekkers 1999a), the temperature-dependent susceptibilities from room temperature up to 280–700 °C and back to room temperature of a loess sample (depth of 14.1 m) and a soil sample (depth of 9.1 m) were measured with a furnace-equipped KLY-3 Kappabridge (Agico Ltd, Brno) at the Palaeomagnetism Laboratory of the Institute of Geology and Geophysics (IGG) in Beijing. Powdered samples were heated and cooled in argon to minimize the possibility of oxidation. The partial heating/cooling method (Van Velzen & Dekkers 1999a) involves separate heating/cooling runs on sets of identical specimens, with different maximum temperatures for each specimen. This makes it possible to characterize the magnetic mineral alterations that occur during heating in each temperature interval (Van Velzen & Dekkers 1999a; Deng *et al.* 2001; Zhu *et al.* 2001).

Hysteresis parameters (such as saturation magnetization M_s, saturation remanence M_{rs}, coercivity B_c and coercivity of remanence B_{cr}) and isothermal remanent magnetization (IRM) acquisition curves of 17 loess samples and 14 soil samples were measured using a Princeton Measurements Corp. Model 2900 MicroMag Alternating Gradient Magnetometer (AGM) at the Palaeomagnetism Laboratory of the IGG. The maximum field applied is 1.5 T. M_s, M_{rs} and B_c were determined after the correction for the paramagnetic contribution identified from the slope at high fields of the hysteresis loops. Samples were then demagnetized in an alternating field (AF) up to 200 mT, and the IRM was imparted from 0 to 1.5 T using the same instrument. Subsequently, the IRM at 1.5 T was demagnetized in a stepwise backfield from 0 to −1.5 T to obtain B_{cr}.

Low-temperature remanence measurements of a soil sample (depth of 10.3 m) were made with a Quantum Design Magnetic Property Measurement System (MPMS-2) at the Institute for Rock Magnetism, University of Minnesota. The sample was first cooled to 20 K in a zero magnetic field (zero-field-cooled, ZFC) environment and then a saturation remanence was imparted by applying a 2.5 T direct (DC) magnetic field. Thermal demagnetization of the ZFC low-temperature remanence was measured in zero field

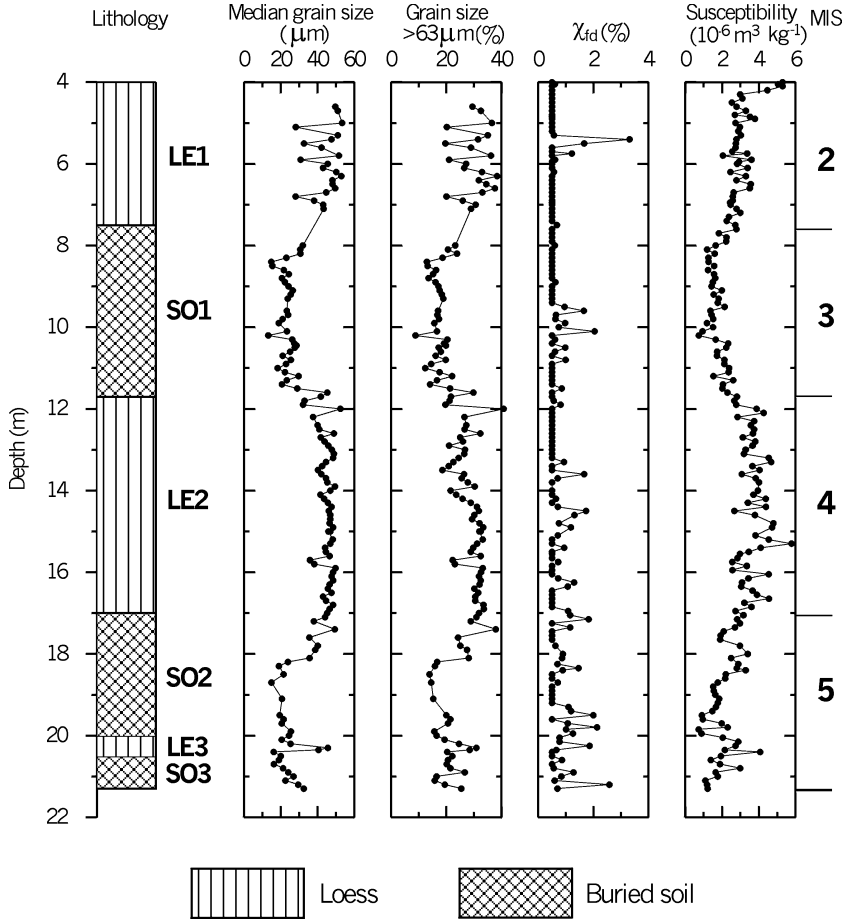

Figure 2 Grain size, lithology, mass specific magnetic susceptibilities and frequency-dependent susceptibility versus depth for the Kurtak section in the southern Siberia. Marine oxygen isotope stages (MIS) are cited from Chlachula *et al.* (1997).

warming to room temperature (300 K). Measurements were made at 5 K intervals. The sample was next cooled from 300 to 20 K in a 2.5 T direct magnetic field (field-cooled, FC). A saturation remanence was induced at 20 K. Then the thermal demagnetization of the FC low-temperature remanence was measured. The first derivatives (dM/dT) of the thermal demagnetization curves of both ZFC and FC low-temperature remanence were calculated in order to better identify changes during sample warming. In addition, another parallel specimen of the soil sample was given a saturation remanence at room temperature (RTSIRM) in a field of 2.5 T. The RTSIRM was cooled to 20 K and then warmed back to room temperature in a zero field.

X-ray diffraction (XRD) analysis of magnetic extracts of a buried soil sample (depth of 9.7 m) was carried out using a computer-controlled Philips PW2273 diffractometer with the following conditions: Cu-Kα, a scattering slit of 1°, continuous scan mode, a scanning speed of 2 deg min^{-1} and a scanning step of 0.02°. The magnetic minerals were extracted by circulating sediment slurry between the polar pieces of a Frantz-type magnetic separator.

4 EXPERIMENTAL RESULTS

4.1 Susceptibility and grain size

The mass-specific magnetic susceptibility profiles reflect changes in lithology between loess and buried soils (Fig. 2). Analogous to the evidence reported by Chlachula *et al.* (1997), the buried soils at Kurtak are characterized by lower susceptibilities with the lowest value of 0.7×10^{-6} m^3 kg^{-1} and a mean value of 1.0×10^{-6} m^3 kg^{-1}, whereas the higher values were found in loess horizons with the highest susceptibility value of 5.8×10^{-6} m^3 kg^{-1} and a mean value of 2.0×10^{-6} m^3 kg^{-1}. These variations mirror the pattern observed in loess sequences in Alaska (Begét *et al.* 1990; Liu *et al.* 1999), and the sand dune sections in northeastern China (Sun & Liu 2000), and are opposite to those found in the classic sections of the Chinese Loess Plateau (e.g. Heller & Evans 1995; Florindo *et al.* 1999).

Loess and buried soils at Kurtak show almost no frequency dependence of susceptibility (Fig. 2). This behaviour is consistent with the Alaskan aeolian deposits (Liu *et al.* 1999) but significantly different from the loess/palaeosols in China (Liu *et al.* 1990; Evans & Heller 1994; Forster *et al.* 1994) and in Bulgaria (Jordanova & Petersen 1999). Frequency-dependent susceptibility is generally considered to be a sensitive indicator of the presence of superparamagnetic (SP) grains produced by *in situ* pedogenesis (Liu *et al.* 1990). Therefore, the low values of frequency dependence of the susceptibility throughout most of the investigated interval could suggest very weak pedogenesis at Kurtak.

Grain size variations at Kurtak are similar to the pattern of typical sections in the Chinese Loess Plateau (Ding *et al.* 1992), i.e. the median grain size of the buried soil is finer than that of the loess (Fig. 2). However, the median grain size and the sand fraction of >63 μm correlate well with the magnetic susceptibility, with correlation

coefficients of $R = 0.76$ and 0.52, respectively. This linear behaviour indicates that coarse fractions make a significant contribution to the magnetic susceptibility.

4.2 High-temperature susceptibility measurements

The representative temperature dependence of magnetic susceptibility curves for a loess and buried soil specimens are shown in Fig. 3. For the soil specimen, the run to 280 °C is almost reversible (Fig. 3a), indicating that magnetic minerals remain basically unchanged below this temperature. However, this run for the loess specimen is not completely reversible: the slightly higher susceptibility values after cooling seem to be caused by an irreversible change at ∼150 °C. This change may be related to surface oxidation of magnetite (Van Velzen & Dekkers 1999b). In the 400 °C run, the heating curves display a bump at ∼280 °C, followed by a decrease in susceptibility (Fig. 3b). The decrease in susceptibility from 280 to 390 °C may result from the thermally induced conversion of some metastable ferrimagnetic maghemite (γ-Fe_2O_3) to weakly magnetic haematite (α-Fe_2O_3) (Oches & Banerjee 1996; Florindo *et al.* 1999; Zhu *et al.* 1999; Deng *et al.* 2000). In this run, the susceptibility values decrease very slowly during cooling (Fig. 3b). Some pronounced differences of the heating curves between loess and buried soil

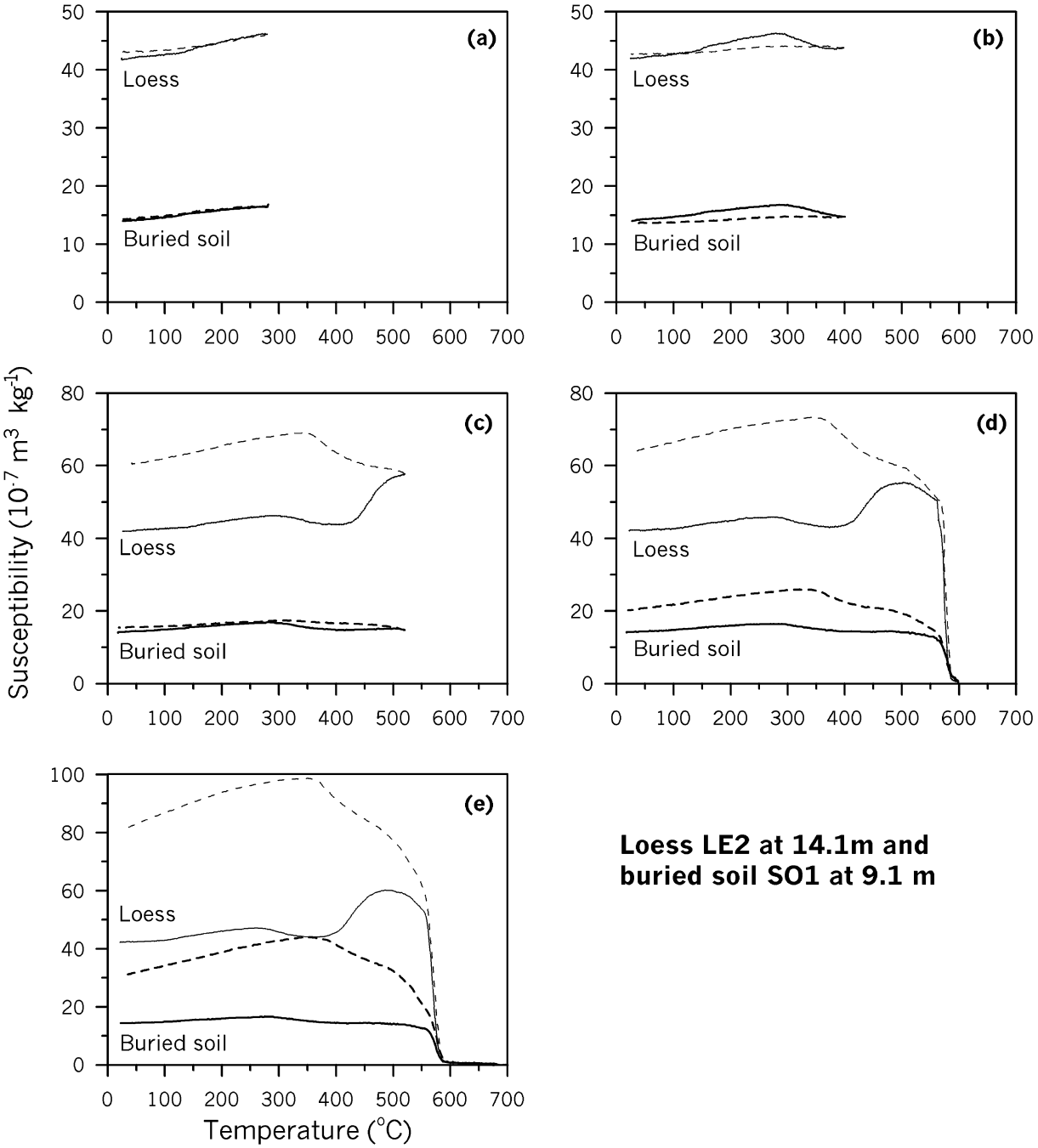

Figure 3 Typical temperature-dependent susceptibility curves. Thick (thin) curves stand for buried soil (loess). Solid (dashed) lines represent heating (cooling) runs.

specimens begin to occur when the highest heating temperatures rise to >520 °C (Figs 3c–e). The cooling cycles show a rapid increase in magnetic susceptibility in the runs to 520, 600 and 700 °C, suggesting significant thermally induced formation of new ferrimagnetic minerals. The heating curves of the 600 and 700 °C runs are alike, although more ferrimagnetic minerals have been produced in the 700 °C run in both soil and loess. A susceptibility hump at ∼500 °C is very pronounced for the loess specimens and significantly muted for the buried soil specimens (Figs 3d and e). The cooling curves show a sharp increase in magnetic susceptibility when cooled below 585 °C (Figs 3d and e). This behaviour is much more pronounced for the loess specimens than for the soil specimens. The susceptibility decreases slowly with temperature when cooled below ∼350 °C. This decrease may be caused by the formation of specific grain sizes that show superparamagnetic behaviour in the range between room temperature and 350 °C (Figs 3d and e).

4.3 IRM acquisition and DC field demagnetization of SIRM

The two samples from the loess unit LE2 and buried soil SO1 yield very similar IRM acquisition curves (Fig. 4). Approximately 90 per cent of the SIRM is acquired below an inducing field of 300 mT. The remanence continues to be acquired above 300 mT, which is generally considered to be the theoretical maximum coercivity for magnetite grains. Therefore, approximately 10 per cent of this remanence is apparently carried by haematite and/or goethite. Two parameters are used to further identify the magnetic mineralogy: the remanent acquisition coercive force (B'_{cr}) (Dankers 1981) and the coercivity of remanence (B_{cr}). These are the applied magnetic fields at which 50 per cent of the eventual SIRM is achieved in the forward direction, and at which the IRM of a previously saturated sample is reduced to zero in the back-field direction, respectively. The loess samples yield $B'_{cr} = 81 \pm 3$ and $B_{cr} = 50 \pm 4$ mT ($N = 14$); the buried soil samples, $B'_{cr} = 79 \pm 5$ and $B_{cr} = 52 \pm 5$ mT ($N = 12$). Both B'_{cr} and B_{cr} values of the loess and buried soil samples fall in low ranges, indicating that all the measured samples have very similar coercivity spectra. This gives B'_{cr}/B_{cr} ratios of 1.6 ± 0.1 for the loess and 1.5 ± 0.1 for the buried soils, respectively. The ratios are close to the result of Dankers (1981). He reports $B'_{cr}/B_{cr} = 1.6 \pm 0.2$ for pure magnetite of many different grain sizes. Therefore, it can be concluded that the magnetic mineralogy in the investigated interval

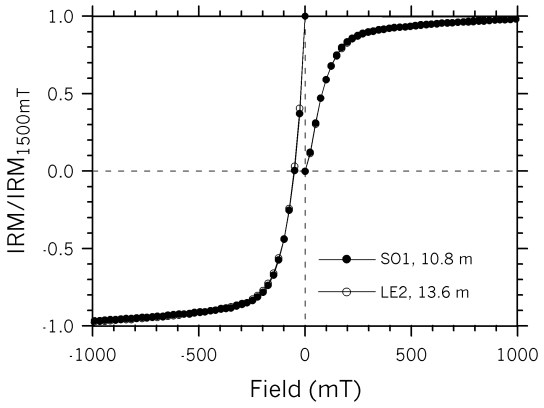

Figure 4 Isothermal remanence magnetization acquisition and DC demagnetization curves for one loess sample and one buried soil sample of the Kurtak section. The curves are obtained in the applied field up to ±1500 mT, which are cut-off at 1000 mT for reasons of clarity.

is dominated by magnetite. In addition, we note that the buried soils show higher B_{cr} values and lower B'_{cr}/B_{cr} ratios than loess units. This behaviour probably suggests that some high-coercivity components make more significant contributions to the magnetic properties of the buried soils than of the loess units at Kurtak.

4.4 Hysteresis measurements

The hysteresis loops are closed in applied fields of 300 mT for loess and of ∼350 mT for buried soils (Fig. 5). We attribute the higher coercivities of the soils to surface oxidation of magnetite grains (Van Velzen & Zijderveld 1995; Van Velzen & Dekkers 1999a) or to hard magnetic phases. The values of M_{rs}/M_s versus B_{cr}/B_c are plotted in a Day diagram (Day *et al.* 1977, Fig. 6). All the loess samples and most of the buried soil samples have low M_{rs}/M_s values and high B_{cr}/B_c values, which indicate that the magnetic mineralogy is dominated by multidomain- (MD-) like magnetite grains. Only three soil samples fall into the pseudo-single-domain (PSD) range. We also note that hysteresis data from the loess horizons tend to be closer to the MD region of the Day plot than those from the buried soil horizons. This evidence may reflect stronger winds during the deposition of loess horizons, which transport coarser magnetite grains responsible for the higher susceptibilities in the loess horizons.

4.5 Low-temperature remanence measurements

Magnetite is demonstrated by remanence losses at the Verwey transition (Fig. 7). This transition is much more pronounced in the *dM/dT* curves (Fig. 7a). On warming a low-temperature remanence, the magnetite contribution is more visible for a zero-field-cooled remanence than for a field-cooled remanence. The decrease during warming of the ZFC remanence can be attributed to SP grains with very low unblocking temperatures (Özdemir *et al.* 1993), while the decrease in the FC remanence is caused by the relaxation of the stabilized remanence (Smirnov & Tarduno 2000). The difference between ZFC and FC curves may be taken as an indication for some oxidation of the magnetite and/or probably in part as the goethite signal. Although goethite is identified less definitively, two factors could suggest a goethite contribution. One is the large difference between FC and ZFC remanences, roughly a factor of 2 at 20 K, and the gradual convergence of the FC and ZFC curves all the way to 300 K (Fig. 7a). The second indication of goethite is the strong increase of RTSIRM on cooling (Fig. 7b) (Jackson, pers. comm., 2000). The relative contributions of goethite, magnetite, and any other possible magnetic phases are difficult to constrain based on the present data. Certainly, the sharp drops around 120 K are attributable to magnetite. The more progressive decay on warming is probably caused by both goethite and SP magnetite, with the former contribution greatly enhanced in the FC curves. The remanence remaining after warming to room temperature also probably comprises contributions from magnetite and goethite, and probably other minerals including haematite and maghemite, concerning which this data set provides little information.

4.6 X-ray diffraction analysis

The XRD spectra obtained reveal the presence of a mixture of magnetite, maghemite and haematite in buried soils (Fig. 8). The XRD analysis further confirms and enhances the interpretation of the high-temperature susceptibility measurements (Fig. 3), which indicate that magnetite is the major contributor to the magnetic susceptibility.

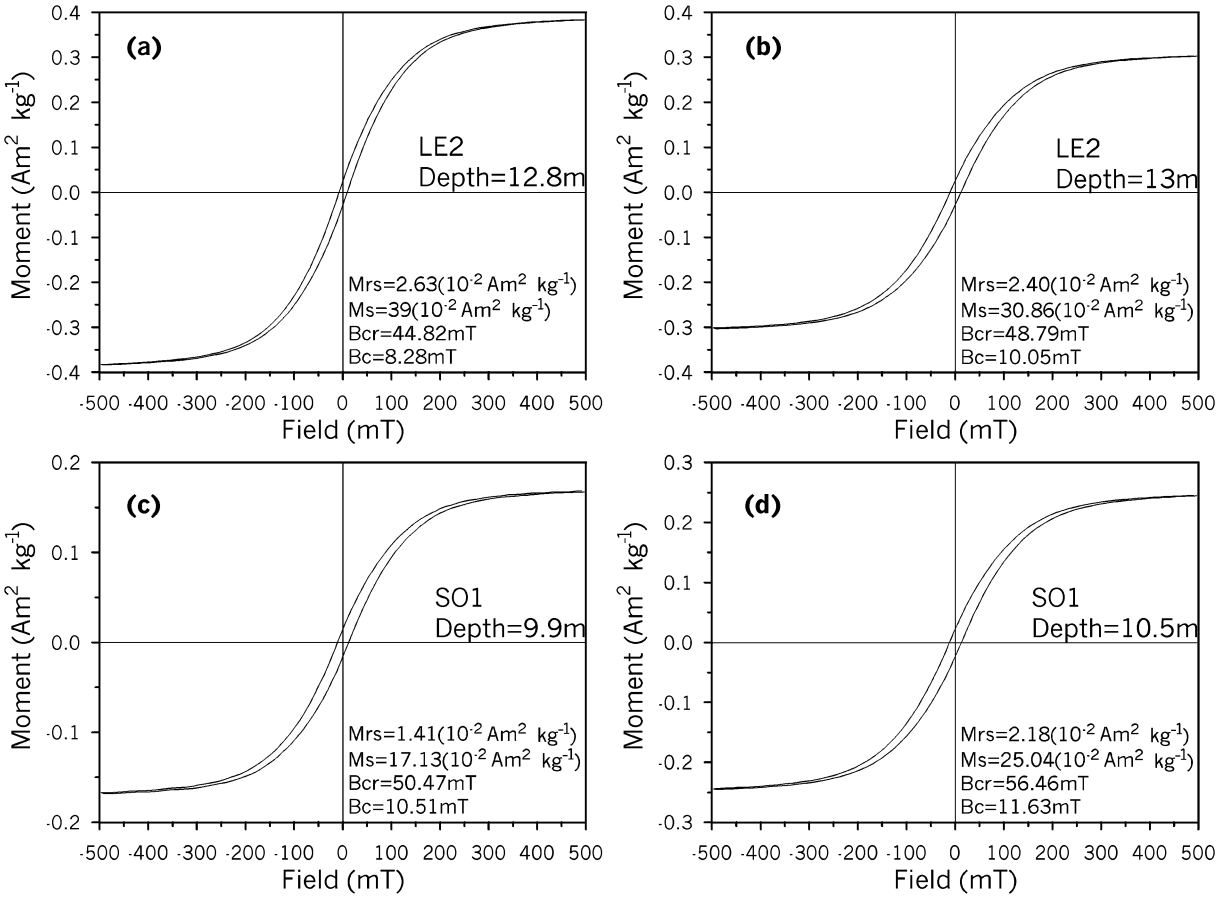

Figure 5 Hysteresis loops for four representative samples of loess (a, b) and buried soil (c, d) after slope correction for the paramagnetic contribution. The hysteresis parameters were measured up to ±1.5 T.

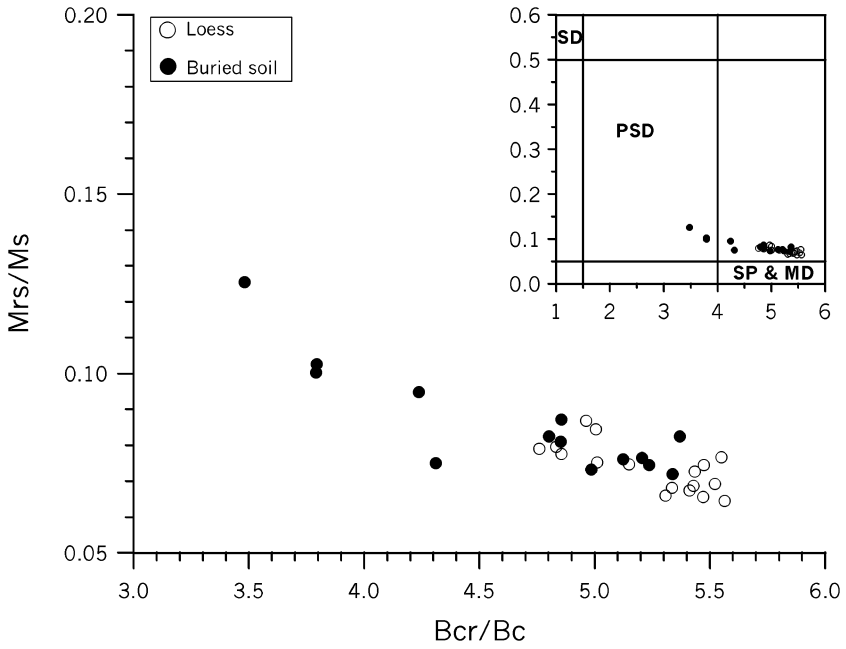

Figure 6 Hysteresis ratios as plotted on a Day *et al.* (1977) diagram for the loess and buried soils at Kurtak.

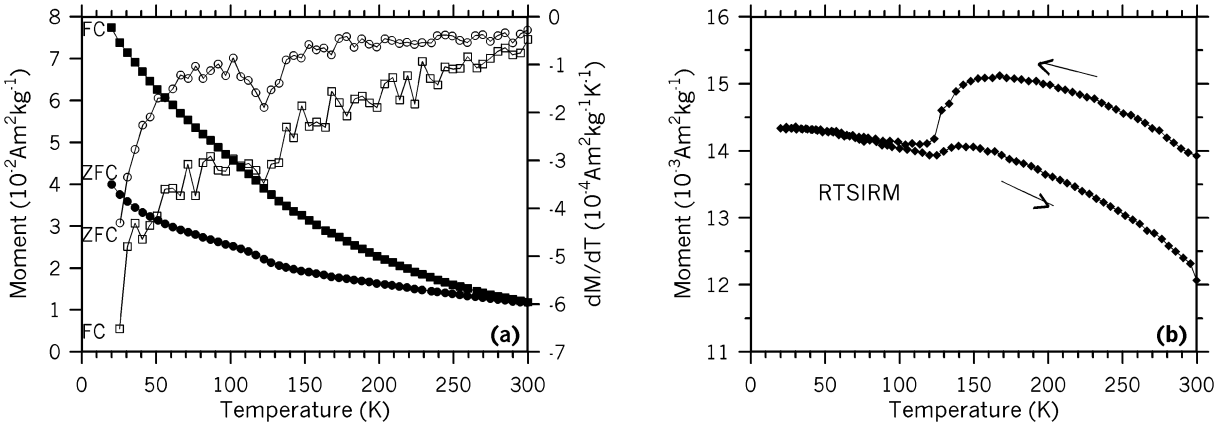

Figure 7 (a) The thermal demagnetization curves of zero-field-cooled (solid circles) and field-cooled (solid squares) low-temperature remanence of a buried soil sample (depth of 10.3 m). The first derivatives (*dM*/*dT*) of demagnetization curves of the ZFC and FC remanence are shown by open circles and open squares, respectively. (b) Cooling and warming the room-temperature saturation remanence (RTSIRM) of the sample.

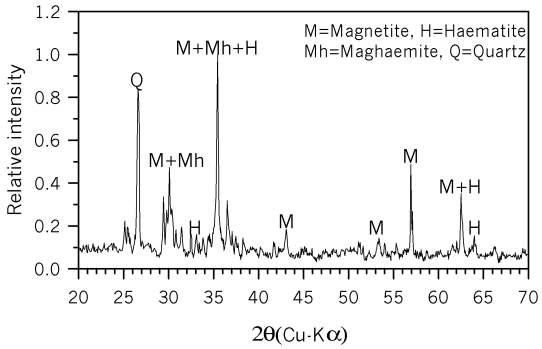

Figure 8 XRD spectrum of magnetic extracts from a buried soil sample (depth of 9.7 m), showing quartz, magnetite, haematite and maghemite in the sediment.

5 DISCUSSION AND CONCLUSIONS

As shown by XRD analysis, magnetite, maghemite and haematite are present in the aeolian deposits at Kurtak (Fig. 8). However, the magnetic mineralogy in both the loess and the buried soils is dominated by magnetite. Some magnetite grains could have been partly maghemitized, as suggested by the depression of the Verwey transition for a buried soil sample (Fig. 7a). The presence of maghemite is suggested by the susceptibility drop between 280 and 390 °C during heating (Figs 3b–e). The IRM acquisition curves (Fig. 4) may indicate that high-coercivity components such as haematite and/or goethite also contribute to the magnetic properties of the loess and buried soils at Kurtak. Low-temperature remanence measurements (Fig. 7) also suggest the possible presence of goethite in the buried soils. Obviously, the magnetic evidence for goethite remains less definitive. Furthermore, XRD spectrum of a buried soil sample (Fig. 8) fails to detect this mineral.

The low-field magnetic susceptibility records of the loess-soil sequence at Kurtak show features similar to those documented in the marine oxygen isotope records (Chlachula *et al.* 1997), indicative of a link between magnetic properties of Siberian aeolian deposits and global climate system changes. However, it is important to note that the stratigraphic variations of susceptibility at Kurtak are anticorrelated to the susceptibility patterns observed at most of the loess sections on the Chinese Loess Plateau, where higher susceptibility values occur in palaeosols and lower values in loesses (e.g. Heller & Liu 1984, 1986; Heller & Evans 1995). Clearly, *in situ* post-depositional alteration by pedogenesis, believed to be the most probable mechanism for magnetic susceptibility enhancement in Chinese loess and palaeosols (Zhou *et al.* 1990; Maher & Thompson 1991; Verosub *et al.* 1993; Zhu *et al.* 1994; Hunt *et al.* 1995), is not applicable at Kurtak.

Importantly, we find there is a significant relationship between the susceptibility and the sand fraction of >63 μm (Fig. 2). This probably suggests that the higher susceptibility in the loess horizons is not associated with the ultrafine minerals but the coarse size fraction. Hysteresis parameters further suggest that magnetic mineralogy is dominated by MD magnetite (Fig. 6), if the data are not biased by the presence of magnetic minerals other than magnetite. The relatively low values of frequency-dependent susceptibility (Fig. 2) also indicate the absence of ultrafine (SP) magnetite grains in loess and buried soils. Since magnetite is almost twice as dense as quartz (magnetite, Fe_3O_4, 5190 kg m^{-3}; quartz, SiO_2, 2650 kg m^{-3}; Evans 2001), giving a diameter ratio of $\sim 2^{1/3} = 1.26$ between quartz and magnetite for the equidimensional grains with the same weight, we can realistically expect that $\sim$63 μm quartz grains have approximately the same weight as $\sim$50 μm magnetite grains. Thus, we suggest that >50 μm magnetite particles make significant contributions to magnetic minerals in the aeolian deposit sequences at Kurtak. Because the quartz particles of >63 μm and magnetite particles of >50 μm cannot be transported over long distances even during intense dust storms, they are mainly transported by saltation or modified saltation over short distances. The region to the north and northeast of the Kurtak section is covered by ice and snow in winter, thus there is less material available to become aeolian dust. Additionally, the dust contributing to aeolian deposits is transported by lower atmospheric circulation (Pye & Zhou 1989), the aeolian dust from the distal western and southwestern provenance is basically negligible because of the influence of the mountains with a mean elevation of approximately 2100 m to the west and southeast of Kurtak. Therefore, it can be reasoned that the deposits at Kurtak chiefly come from a local source, i.e. from local river channels by valley winds. Therefore, our results provide a strong support for the concept that the Siberian aeolian deposits are pre dominantly of local provenance (Chlachula *et al.* 1997). They reached this conclusion based on the fact that the Kurtak loess samples analysed by scanning electron microscopy exhibit angular shapes and unweathered surface morphology for most grains.

At Kurtak, the loess horizons could be considered as an alternation of differently coloured aleurites and loams with abundant

Fe-concretions, Mn-mottling and gleying; and the buried soils are mainly composed of chernozem soils with weakly developed humic horizons (Chlachula 2001; Chlachula *et al.* 1997; Matasova *et al.* 2001). These pedogenetic characteristics indicate a relatively cool and humid periglacial climate during soil formation. The climate at Kurtak favoured gleying of the soils during interstadial and interglacial periods, leading to degradation and destruction of magnetite and maghemite grains and to formation of weakly magnetic α-ferric oxyhydroxides, i.e. goethite. The low-temperature remanence measurements (Fig. 7) suggest that goethite is probably present in the buried soils, but it was not unambiguously identified by XRD analysis (Fig. 8). Therefore, the lower susceptibility values of the buried soil horizons (SO1, SO2, SO3) at Kurtak could also be partly caused by gleying or waterlogging processes during interstadial and interglacial intervals.

In summary, our results presented here further suggest that, on the one hand, the variability of local valley winds is chiefly responsible for the observed susceptibility characteristics; on the other hand, gleying or waterlogging in the cooler and more humid interstadial and interglacial times is probably another important factor resulting in the lower susceptibility values in the buried soil horizons at Kurtak.

ACKNOWLEDGMENTS

This work was supported by the National Natural Science Foundation of China (grant no 40074016) and RFBR-NFNS (grant no 99-05-39077). We wish to thank Dr Mike Jackson for carrying out the low-temperature experiments. The great assistance given by our colleagues at the palaeomagnetism laboratory of the Institute of Geology and Geophysics, Chinese Academy of Sciences is gratefully acknowledged.

REFERENCES

Arkhipov, S.A., Gnibidenko, Z.N., Zykina, V.S., Krukover, A.A. & Shelkoplays, V.N., 1992. Geological setting and common strategy of chronostratigraphic investigations of the Kurtak archeological region, in, *Palaeoecology and Distribution of Ancient Men in Northern Asia and America,* pp. 10–15, ed. Drozdov, N., Krasnoyarsk, Russia (in Russian).

Begét, J.E., Stone, D.B. & Hawkins, D.B., 1990. Paleoclimatic forcing of magnetic susceptibility variations in Alaskan loess during the late Quaternary, *Geology,* **18,** 40–43.

Chlachula, J., 2001. Pleistocene climate change, natural environments and palaeolithic occupation of the Yenisei area, south-central Siberia, *Quat. Int.,* **80–81,** 101–130.

Chlachula, J., Rutter, N.W. & Evans, M.E., 1997. A late Quaternary loess–paleosol record at Kurtak, southern Siberia, *Can. J. Earth Sci.,* **34,** 679–686.

Chlachula, J., Evans, M.E. & Rutter, N.W., 1998. A magnetic investigation of a Late Quaternary loess/palaeosol record in Siberia, *Geophys. J. Int.,* **132,** 128–132.

Dankers, P., 1981. Relationship between median destructive field and remanent coercive forces for dispersed natural magnetite, titanomagnetite and hematite, *Geophys. J. R. astr. Soc.,* **64,** 447–461.

Day, R.M., Fuller, M. & Schmidt, V.A., 1977. Hysteresis properties of titanomagnetites: grain size and compositional dependence, *Phys. Earth planet. Inter.,* **13,** 260–267.

Deng, C., Zhu, R., Verosub, K.L., Singer, M.J. & Yuan, B., 2000. Paleoclimatic significance of the temperature-dependent susceptibility of Holocene loess along a NW–SE transect in the Chinese loess plateau, *Geophys. Res. Lett.,* **27,** 3715–3718.

Deng, C., Zhu, R., Jackson, M.J., Verosub, K.L. & Singer, M.J., 2001. Variability of the temperature-dependent susceptibility of the Holocene eolian deposits in the Chinese loess plateau: a pedogenesis indicator, *Phys. Chem. Earth (A),* **26,** 873–878.

Ding, Z.L., Rutter, N.W., Han, J.M. & Liu, T.S., 1992. A coupled environmental system formed at about 2.5 Ma in East Asia, *Palaeogeog. Palaeoclimat. Palaeoecol.,* **94,** 223–242.

Evans, M.E., 2001. Magnetoclimatology of aeolian sediments, *Geophys. J. Int.* **144,** 495–497.

Evans, M.E. & Heller, F., 1994. Magnetic enhancement and palaeoclimate: study of a loess/palaeosol couplet across the Loess Plateau of China, *Geophys. J. Int.,* **117,** 257–264.

Evans, M.E. & Heller, F., 2001. Magnetism of loess/paleosol sequences: recent developments, *Earth Sci. Rev.,* **54,** 129–144.

Florindo, F., Zhu, R., Guo, B., Yue, L., Pan, Y. & Speranza, F., 1999. Magnetic proxy climate results from the Duanjiapo loess section, southernmost extremity of the Chinese loess plateau, *J. geophys. Res.,* **104,** 645–659.

Forster, T., Evans, M.E. & Heller, F., 1994. The frequency dependence of low-field susceptibility in loess sediments, *Geophys. J. Int.,* **118,** 636–642.

Frechen, M. & Yamskikh, A.F., 1999. Upper Pleistocene loess stratigraphy in the southern Yenisei Siberia area, *J. geol. Soc. Lond.,* **156,** 515–525.

Heller, F. & Evans, M.E., 1995. Loess magnetism, *Rev. Geophys.,* **33,** 211–240.

Heller, F. & Liu, T.S., 1984. Magnetism of Chinese loess deposits, *Geophys. J. R. astr. Soc.,* **77,** 125–141.

Heller, F. & Liu, T.S., 1986. Paleoclimatic and sedimentary history from magnetic susceptibility of loess in China, *Geophys. Res. Lett.,* **13,** 1169–1172.

Hunt, C.P., Banerjee, S.K., Han, J., Solheid, P.A., Oches, E., Sun, W. & Liu, T., 1995. Rock-magnetic proxies of climate change in the loess–paleosol sequences of the western Loess Plateau of China, *Geophys. J. Int.,* **123,** 232–244.

Jordanova, D. & Petersen, N., 1999. Paleoclimatic record from a loess-soil profile in northeastern Bulgaria—I. Rock magnetic properties, *Geophys. J. Int.,* **138,** 520–532.

Kukla, G., Heller, F., Liu, X.M., Xu, T.C., Liu, T.S. & An, Z.S., 1988. Pleistocene climates in China dated by magnetic susceptibility, *Geology,* **16,** 811–814.

Liu, X.M., Liu, T.S., Heller, F. & Xu, T.C., 1990. Frequent-dependent susceptibility of loess and Quaternary paleoclimate (in Chinese with English abstract), *Quat. Sci.,* **1,** 42–50.

Liu, X.M., Hesse, P., Rolph, T. & Begét, J.E., 1999. Properties of magnetic mineralogy of Alaskan loess: evidence for pedogenesis, *Quat. Int.,* **62,** 93–102.

Maher, B.A., 1998. Magnetic properties of modern soils and Quaternary loessic paleosols: paleoclimatic implications, *Palaeogeog. Palaeoclimat. Palaeoecol.,* **137,** 25–54.

Maher, B.A. & Thompson, R., 1991. Mineral magnetic record of the Chinese loess and paleosols, *Geology,* **19,** 3–6.

Matasova, G.G., Kazansky A. & Zykina, V.S., 2000. Petromagnetic characteristics of Kurtak key loess–paleosol section (Middle Siberia) and their significance for climatic reconstructions, in, *Problems of Reconstructions of Climate and Environment in Holocene and Pleistocene of Siberia, IAE SB RAS, Issue 2,* pp. 313–331, ed. Derevjanko, A., Russian Academy of Sciences, Novosibirsk, Russia (in Russian).

Matasova, G., Petrovsky, E., Jordanova, N., Zykina, V. & Kapicka, A., 2001. Magnetic study of Late Pleistocene loess/palaeosol sections from Siberia: palaeoenvironmental implications, *Geophys. J. Int.,* **147,** 367–380.

Oches, E.A. & Banerjee, S.K., 1996. Rock-magnetic proxies of climate change from loess–paleosol sediments of the Czech Republic, *Stud. Geophys. Geodaet.,* **40,** 287–300.

Özdemir, Ö., Dunlop, D.J. & Moskowtiz, B.M., 1993. The effect of oxidation on the Verwey transition in magnetite, *Geophys. Res. Lett.,* **20,** 1671–1674.

Pye, K. & Zhou, L.P., 1989. Late Pleistocene and Holocene aeolian dust deposition in North China and the Northwest Pacific Ocean, *Palaeogeog. Palaeoclimat. Palaeoecol.,* **73,** 11–23.

Smirnov, A.V. & Tarduno, J.A., 2000. Low-temperature magnetic properties of pelagic sediments (Ocean Drilling Program Site 805C): tracers of maghemitization and magnetic mineral reduction, *J. geophys. Res.,* **105,** 16 457–16 471.

Sun, J.M. & Liu, T.S., 2000. Multiple origins and interpretations of the magnetic susceptibility signal in Chinese wind-blown sediments, *Earth planet. Sci. Lett.,* **180,** 287–296.

Van Velzen, A.J. & Dekkers, M.J., 1999a. The incorporation of thermal methods in mineral magnetism of loess–paleosol sequences: a brief overview, *Chinese Sci. Bull.,* **44,** (suppl. 1), 53–63.

Van Velzen, A.J. & Dekkers, M.J., 1999b. Low-temperature oxidation of magnetite in loess–paleosol sequences: a correction of rock magnetic parameters, *Stud. Geophys. Geodaet.,* **43,** 357–375.

Van Velzen, A.J. & Zijderveld, J.A.D., 1995. The effects of weathering on single domain magnetite in Early Pliocene marine marls, *Geophys. J. Int.,* **121,** 267–278.

Verosub, K.L., Fine, P., Singer, M.J. & TenPas, J., 1993. Pedogenesis and paleoclimate: interpretation of the magnetic susceptibility record of Chinese loess–paleosol sequences, *Geology,* **21,** 1011–1014.

Volkov, I.A. & Zykina, V.S., 1984. Stratigraphy of the Quaternary loess deposits of the Novosibirsk Priobie, in, *Proc. 11th INQUA Congress,* pp. 17–21, ed. Arkhipov, V.S., Russian Academy of Sciences, Novosibirsk (in Russian).

Zhou, L.P., Oldfield, F., Wintle, A.G., Robinson, S.G. & Wang, J.T., 1990. Partly pedogenic origin of magnetic variations in Chinese loess, *Nature,* **346,** 737–739.

Zhu, R.X., Wu, H.N., Li, C.J., Ding, Z.L. & Guo, Z.T., 1994. Magnetic property of Chinese loess and its paleoclimate significance, *Sci. China B,* **38,** 238–244.

Zhu, R.X., Lin, M. & Pan, Y.X., 1999. History of the temperature-dependence of susceptibility and its implications: Preliminary results along an E–W transect of the Chinese Loess Plateau, *Chinese Sci. Bull.,* **44,** (suppl. 1), 81–86.

Zhu, R.X., Kazansky, A., Matasova, G., Guo, B., Zykina, V., Petrovsky, E. & Jordanova, N., 2000. Rock-magnetic investigation of Siberia loess and its implication, *Chinese Sci. Bull.,* **45,** 2192–2197.

Zhu, R., Deng, C. & Jackson, M.J., 2001. A magnetic investigation along a NW–SE transect of the Chinese Loess Plateau and its implications, *Phys. Chem. Earth A,* **26,** 867–872.